PAUSED, a Putative Exportin-t, Acts Pleiotropically in Arabidopsis Development But Is Dispensable for Viability[1] [w]

Junjie Li and Xuemei Chen*

Waksman Institute, Rutgers University, Piscataway, New Jersey 08854 (J.L., X.C.)

Exportin-t was first identified in humans as a protein that mediates the export of tRNAs from the nucleus to the cytoplasm. Mutations in Los1p, the *Saccharomyces cerevisiae* exportin-t homolog, result in nuclear accumulation of tRNAs. Because no exportin-t mutants have been reported in multicellular organisms, the developmental functions of exportin-t have not been determined. Here, we report the isolation and characterization of two Arabidopsis exportin-t mutants, *paused-5* and *paused-6*. The mutant phenotypes indicate that exportin-t acts pleiotropically in plant development. In particular, *paused-5* and *paused-6* result in delayed leaf formation during vegetative development. The two *paused* mutations also cause the transformation of reproductive organs into perianth organs in the *hua1-1 hua2-1* background, which is partially defective in reproductive organ identity specification. The floral phenotypes of *hua1-1 hua2-1 paused* mutants resemble those of mutations in the floral homeotic gene *AGAMOUS*. Moreover, *paused-5* enhances the mutant phenotypes of two floral meristem identity genes, *LEAFY* and *APETALA1*. The developmental defects caused by *paused* mutations confirm the important roles of exportin-t in gene expression in multicellular organisms. In addition, a *paused* null allele, *paused-6*, is still viable, suggesting the presence of redundant tRNA export pathway(s) in Arabidopsis.

In plants, postembryonic development results from the activities of the apical meristems. The shoot apical meristem (SAM) generates leaves during the vegetative stage of plant development and floral meristems during reproductive development. In Arabidopsis, four types of floral organs, sepal, petal, stamen, and carpel, are produced by a floral meristem in four concentric rings, or whorls. The identities of the four floral organ types are specified by the combinatorial activities of four classes of floral homeotic genes known as A, B, C, and *SEPALLATA* genes (for review, see Theissen and Saedler, 2001; Lohmann and Weigel, 2002). *AGAMOUS* (*AG*), a class C gene, is a master regulator of reproductive organ identities. Severe loss-of-function mutations in *AG* result in the transformation of reproductive organs into perianth organs (Bowman et al., 1989). In addition, *AG* acts in the proper termination of floral meristem activity such that flowers are determinate structures. This *AG* activity results from its ability to repress the stem cell maintenance gene *WUSCHEL* (*WUS*) in the center of flowers (Lenhard et al., 2001; Lohmann et al., 2001).

Several new genes that also act in reproductive organ identity and floral determinacy specification were identified from two genetic screens in sensitized backgrounds. In a genetic screen in the *ag-4* background, recessive mutations in *HUA1* and *HUA2* were found to enhance the phenotypes of the weak *ag-4* allele such that *ag-4 hua1-1 hua2-1* flowers resemble severe *ag* mutants, such as *ag-1*, *ag-2*, or *ag-3* (Chen and Meyerowitz, 1999). The *hua1-1 hua2-1* double-mutant flowers have occasional petaloid stamens and gynoecia with partial sepal character (Chen and Meyerowitz, 1999; Chen et al., 2002; Western et al., 2002), phenotypes that indicate partial loss of class C activity. In a genetic screen in the *hua1-1 hua2-1* background, extragenic, recessive mutations in three *HUA ENHANCER* (*HEN*) loci, *HEN1*, *HEN2*, and *HEN4*, were found to enhance the weak *hua1-1 hua2-1* phenotypes to severe *ag*-like phenotypes, suggesting that the *HEN* genes also act in reproductive organ identity and floral determinacy specification (Chen et al., 2002, Cheng et al., 2003; Western et al., 2002).

Among the newly identified *HUA* and *HEN* genes, *HUA1*, *HUA2*, *HEN2*, and *HEN4* appear to promote *AG* pre-mRNA processing. Mutations in these genes result in the accumulation of *AG* transcripts containing part of the large *AG* second intron (Cheng et al., 2003). HUA1 is a nuclear RNA-binding protein (Li et al., 2001) and interacts with HEN4, a protein with KH-type RNA-binding motifs (Cheng et al., 2003). *HUA2* encodes a protein with motifs found in transcription coactivators and nuclear RNA-processing proteins (Chen and Meyerowitz, 1999; Cheng et al., 2003). *HEN2* encodes a protein with similarity to *Saccharomyces cerevisiae* Dob1p (Mtr4p), a putative

[1] This work was supported by the National Institute of Health (grant no. 1–R01–GM–61146 to X.C.).

[w] The online version of this article contains Web-only data. The supplemental material is available at http://www.plantphysiol.org.

* Corresponding author; e-mail xuemei@waksman.rutgers.edu; fax 732–445–5735.

Article, publication date, and citation information can be found at www.plantphysiol.org/cgi/doi/10.1104/pp.103.023291.

RNA helicase (Western et al., 2002). *HEN1* differs from other *HUA* and *HEN* genes in that it does not appear to be required for *AG* pre-mRNA processing. Two recessive mutations in *HEN1* result in no or reduced accumulation of microRNAs (Park et al., 2002; W. Park and X. Chen, unpublished data), suggesting that HEN1 acts in microRNA metabolism. The fact that *hua1-1 hua2-1 hen1-1* flowers show *ag*-like phenotypes (Chen et al., 2002) suggests that a microRNA(s) acts in reproductive organ identity and floral determinacy specification.

In this report, we describe two recessive mutations in a locus that we initially named *HUA ENHANCER 5* (*HEN5*), *hen5-1* and *hen5-2*, which cause stamen-to-petal and carpel-to-sepal transformation in the *hua1-1 hua2-1* background. We show that *HEN5* is identical to *PAUSED* (*PSD*), a gene previously identified as a regulator of developmental phase transitions (Telfer et al., 1997). We have renamed *hen5-1* and *hen5-2* as *psd-5* and *psd-6*, respectively. We show that *PSD* is required for the proper function of not only the SAM, but also the floral meristems and floral organ primordia. We demonstrate that *PSD* is required for the normal accumulation of *AG* mRNA and protein.

PSD encodes the only protein in the Arabidopsis genome with significant similarity to human exportin-t and yeast Los1p, which are nuclear export receptors of tRNA (Arts et al., 1998; Hellmuth et al., 1998; Kutay et al., 1998). All three proteins have a conserved Ran-binding domain, a signature of the importin-β protein family (Görlich et al., 1997), at the N terminus of the proteins (see below). Ran is a small GTPase and is a crucial component in many nucleocytoplasmic transport processes (for review, see Görlich and Kutay, 1999; Kuersten et al., 2001). Members of the importin-β family can bind Ran and many act in nucleocytoplasmic transport (for review, see Görlich and Kutay, 1999; Cullen, 2000; Grosshans et al., 2000). Despite the critical function of Los1p in nucleocytoplasmic transport of tRNAs, *los1* mutants are viable (Hurt et al., 1987), suggesting the presence of redundant tRNA export pathways in yeast. Exportin-5, another mammalian importin-β protein, has been recently demonstrated to also serve as a tRNA export receptor (Bohnsack et al., 2002; Calado et al., 2002). We demonstrate that *psd-6* is a null allele with undetectable *PSD* mRNA but is still viable and fertile. Therefore, exportin-t, which appears to be dispensable in yeast, is also dispensable in a multicellular organism for viability, suggesting that redundant tRNA export pathway(s) must exist. However, the pleiotropic phenotypes of *psd* mutants suggest that exportin-t is required for multiple developmental pathways in Arabidopsis.

RESULTS

PSD Is Required for the Proper Activities of the SAM

We isolated the *psd-5* mutation from the *hua1-1 hua2-1* mutagenesis screen as a recessive mutation that enhanced the weak *hua1-1 hua2-1* loss-of-C-function phenotypes. The *psd-5* allele was later segregated away from the *hua1-1 hua2-1* background and was found to exhibit a vegetative phenotype on its own. While a wild-type SAM continues to generate leaves on its flanks during vegetative development, leaf formation was variably delayed in *psd-5*. In most *psd-5* plants, the leaf-generating activity of the SAM appeared to be compromised such that fewer leaves were formed than wild type in the same period of time (Fig. 1, A and B). In approximately 17% of the plants, no leaf or only one leaf was generated at d 15 after the transfer of the *psd-5* seeds to the growth

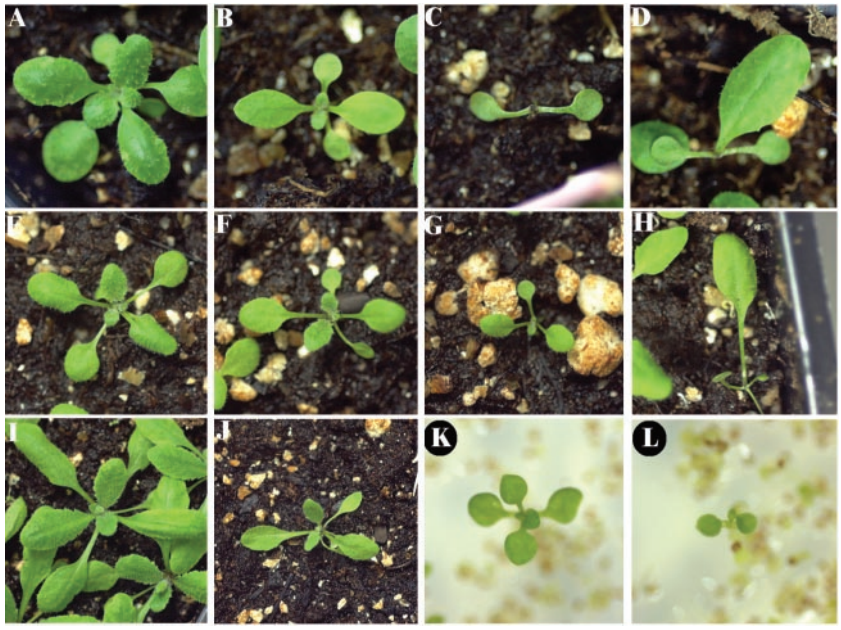

Figure 1. *psd* phenotypes in seedlings. A, A 15-d-old Landsberg *erecta* (L*er*) plant. B, A 15-d-old *psd-5* plant with fewer true leaves than wild type at the same stage. C, A 15-d-old *psd-5* plant with no true leaves. D, A 15-d-old *psd-5* plant with a terminal leaf. E, A 14-d-old Columbia (Col) plant. F and G, 14-d-old *psd-6* plants with fewer true leaves than Col. One cotyledon was absent in G. H, A 20-d-old *psd-6* plant with a terminal leaf. I, A 20-d-old F_1 plant from a cross between Col and L*er*. J, A 20-d-old F_1 plant from a cross between *psd-5* and *psd-6*. Fewer rosette leaves are found than the corresponding wild type (I) at the same stage. K, A 13-d-old *psd-5 hua2-1* (L*er*) transgenic seedling containing pPZP211-HEN5p3/4 showing normal true leaf formation. L, A 13-d-old *psd-5 hua2-1* (L*er*) transgenic seedling containing pPZP-*35S-green fluorescent protein* (*GFP*) showing the *psd-5* phenotype. The magnification in K and L is different from that in A through J.

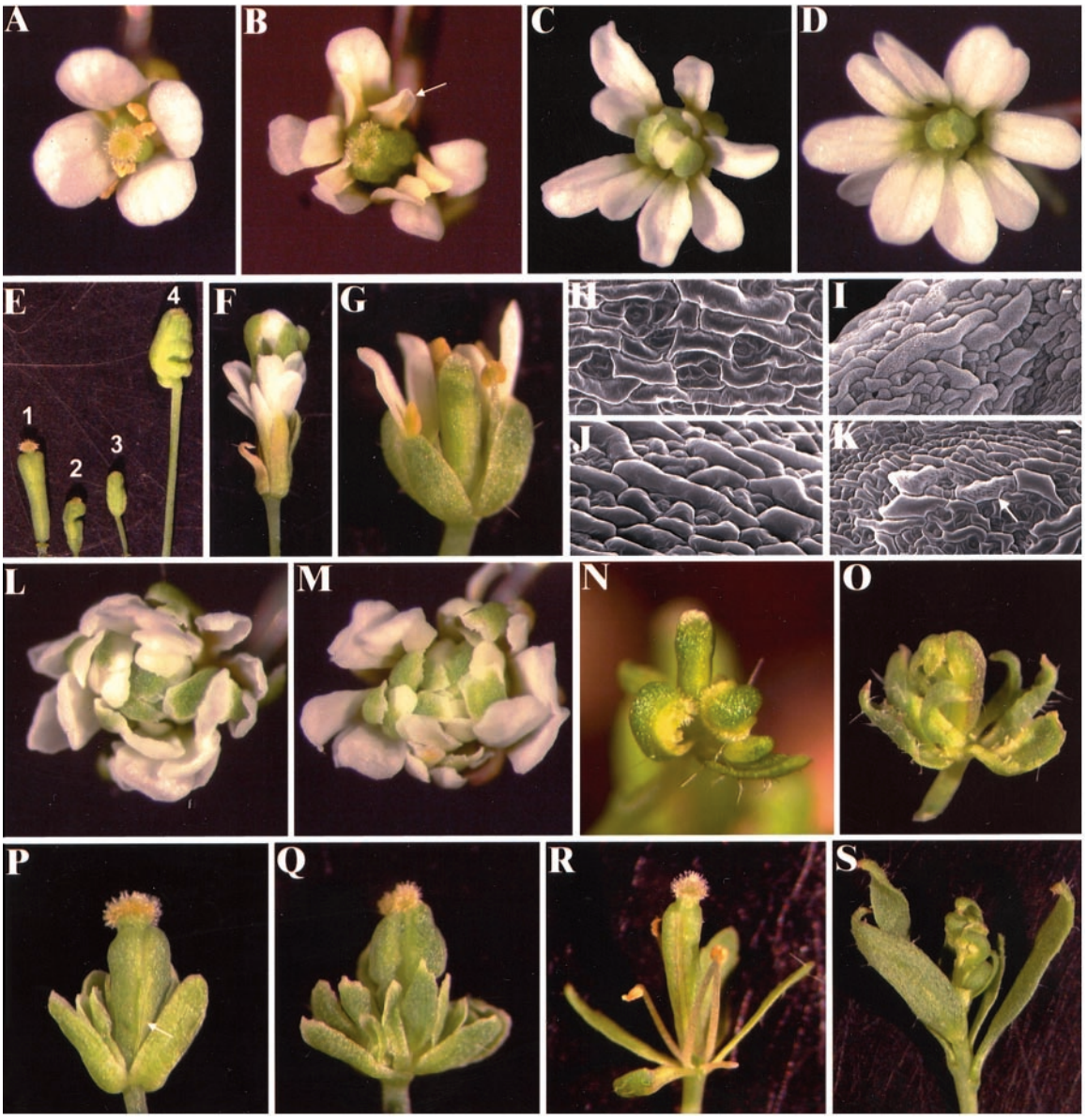

Figure 2. Floral phenotypes of *psd* mutants and interactions with mutations in A, B, and C genes. A, A *hua1-1 hua2-1* (Col) flower. B, An early *hua1-1 hua2-1 psd-5* flower with petals instead of stamens in the third whorl (arrow). C, A late *hua1-1 hua2-1 psd-5* flower with petals in the third whorl and an additional flower in the fourth whorl. D, A *hua1-1 hua2-1 psd-6* (Col) flower showing stamen-to-petal transformation in the third whorl. E, Comparison of *hua1-1 hua2-1* (1), *hua1-1 hua2-1 psd-5* (2), and *hua1-1 hua2-1 psd-6* (3 and 4) gynoecia. F, A *hua1-1 hua2-1 psd-6* flower with an internal flower in the fourth whorl. G, A *psd-5* flower with normal floral organ types. H and I, Abaxial surfaces of the base of a *hua1-1 hua2-1* (H) and a *hua1-1 hua2-1 psd-5* valve (I). J and K, Abaxial surfaces of the apical portion of an L*er* (J) and a *psd-5* valve (K). The *psd-5* valve has a few cells with typical sepal epicuticular striations (arrow). L, A *hua1-1 hua2-1 ag-1* flower. M, A *hua1-1 hua2-1 psd-5 ag-1* flower. N, A *hua1-1 hua2-1 ap2-2* flower. O, A *hua1-1 hua2-1 psd-5 ap2-2* flower. P, A *hua1-1 hua2-1 pi-3* flower with filaments (arrow) in the third whorl. Q, A *hua1-1 hua2-1 psd-5 pi-3* flower with sepals in the third whorl. R, A *hua1-1 hua2-1 ap1-1* flower. S, A *hua1-1 hua2-1 psd-5 ap1-1* "flower" with leaf-like organs in a spiral phyllotaxy, and an internal terminal structure with carpel character. Size bars in H through K = 10 μm.

room (Fig. 1, C and D). At the time of bolting, there were fewer rosette leaves produced in *psd-5* plants (data not shown). After the cloning of the *PSD* gene (see below), we identified another mutant, *psd-6*, which contained a T-DNA insertion in the *PSD* coding region from the Salk T-DNA collection. *psd-6*, which was from a different ecotype, exhibited similar phenotypes as *psd-5* (Fig. 1, E–H), although the frequency of plants with no or only 1 leaf at d 15 was only 4%. These vegetative phenotypes were similar to those of previously described *psd* mutants (Telfer et al., 1997). The layered structure of the SAM is

abnormal in *psd* mutants, and *psd* seedlings appear to contain dead cells at the meristem center (Telfer et al., 1997). The SAM defects may lead to the observed delay in leaf appearance in *psd* plants (Telfer et al., 1997). Thus, *PSD* is required for the proper activity of the SAM.

psd Mutations Result in Floral Organ Identity and Floral Determinacy Defects

In the *hua1-1 hua2-1* background, *psd-5* resulted in stamen-to-petal and carpel-to-sepal transformation in the flower (Fig. 2, A–C), whereas *hua1-1 psd-5* or *hua2-1 psd-5* flowers were indistinguishable from *psd-5* flowers, which were largely normal (Fig. 2G) except for reduced fertility. *hua1-1 hua2-1 psd-5* flowers had petals in the third whorl and gynoecia with smaller and irregularly shaped ovary in the fourth whorl (Fig. 2, B and E). Occasionally in late-arising flowers, additional flowers appeared in the center (Fig. 2C), suggesting loss of floral determinacy. Scanning electron microscopy (SEM) showed that valve epidermal cells throughout *hua1-1 hua2-1 psd-5* ovaries had epicuticular striations that resembled sepal instead of valve epidermal cells (Fig. 2, H and I), whereas cells with sepal characteristics were only found at the apical portion of *hua1-1 hua2-1* valves (Chen et al., 2002; Western et al., 2002). Furthermore, although *psd-5* single mutant flowers were apparently normal (Fig. 2G), occasional valve cells with epicuticular striations could be found in the apical portion of the *psd-5* ovaries (Fig. 2K). Cells with such sepal characteristics were never found in wild-type ovaries (Fig. 2J). In summary, *psd-5* exhibited extremely weak loss-of-C function defects on its own and enhanced the partial loss-of-C function defects of the *hua1-1 hua2-1* mutants.

Another allele, *psd-6*, was isolated from the Salk T-DNA collection and was in the Col background. *psd-6* single-mutant flowers did not display any floral homeotic phenotypes. The *psd-6* allele was crossed into *hua1-1 hua2-1* (Col), a strain in which the *hua1-1* and *hua2-1* mutations were introgressed into the Col background to determine if this *psd* allele also behaved similarly to *psd-5*. The flowers of *hua1-1 hua2-1* (Col) usually had normal stamens (Fig. 2A) and occasionally had petaloid stamens in the third whorl. The *hua1-1 hua2-1 psd-6* flowers had petals in the third whorl (Fig. 2D) and gynoecia with elongated gynophores or another flower in the fourth whorl (Fig. 2, E and F). We also crossed *psd-6* into *hua1-1 hua2-1* in the L*er* background and the F_2 triple mutants displayed floral phenotypes similar to those of *hua1-1 hua2-1 psd-5* or *hua1-1 hua2-1 psd-6* in the Col background (data not shown). Thus, the two *psd* alleles exhibit similar defects in organ identity and floral determinacy and reveal a requirement for *PSD* in floral patterning.

PSD Is Most Probably the Ortholog of Human Exportin-t

To better understand the molecular basis of the *psd* mutant phenotypes, a map-based cloning approach was used to identify the *PSD* gene. *PSD* was mapped to a 27-kb region at the south end of chromosome I on the bacterial artificial chromosome (BAC) F28P22 (Fig. 3A). Sequencing four genes in this region revealed a single nucleotide deletion in the ninth exon of the gene At1g72560 (Fig. 3A). The deletion of a G is predicted to cause a premature stop codon 11 bp after the mutation site. Therefore, At1g72560 is likely the *PSD* gene. To confirm this, a 7-kb genomic fragment surrounding the coding region of At1g72560 was amplified by PCR and cloned into the plant expression vector pPZP211. The resulting construct pPZP211-HEN5p3/4 and another unrelated construct pPZP211-*35S-GFP* were transformed into *psd-5 hua2-1* plants. All 30 transgenic plants containing pPZP211-HEN5p3/4 had normal true leaf initiation or appearance (Fig. 1K). In contrast, transgenic plants containing pPZP211-*35S-GFP* exhibited similar leaf initiation defects to those of *psd-5* (Fig. 1L). Thus, At1g72560 complements the *psd* mutant phenotypes.

To further confirm that At1g72560 is *PSD*, we obtained a T-DNA insertion line, which we later named *psd-6*, from the Salk T-DNA collection. We verified that this line had a T-DNA inserted in the first exon of the At1g72560 gene (Fig. 3A). Compared with wild-type Col plants, these plants had a slower rate of leaf appearance, fewer rosette leaves, and lighter colored leaves (Fig. 1, F–H), phenotypes also exhibited by *psd-5* plants. This T-DNA insertion line was kanamycin sensitive, probably due to silencing of the *NPTII* gene in the T-DNA. To confirm that the phenotypes observed were due to a T-DNA insertion in *PSD* rather than another mutation in the background, we crossed this line with *psd-5*. The F_1 plants showed the *psd* phenotypes, in contrast to the F_1 plants that resulted from crosses between Col and L*er* plants (Fig. 1, I and J). Therefore, the T-DNA mutant is another *psd* allele, which we named *psd-6*. When we introduced this mutation into the *hua1-1 hua2-1* (Col) background, the flowers of the resulting triple-mutant plants had phenotypes similar to *hua1-1 hua2-1 psd-5*: petals in the third whorl instead of stamens, gynoecia with elongated gynophores, or another flower in the center (Fig. 2, D–F).

A *PSD* cDNA was isolated by reverse transcription-PCR from inflorescence tissue. The gene contained 13 exons and 12 introns (Fig. 3A). The predicted PSD protein has 988 amino acids and shares 27% identity and 48% similarity to human exportin-t, and 21% identity and 41% similarity to yeast Los1p throughout the proteins (Fig. 3B). Human exportin-t shares 19% identity and 41% similarity to Los1p. Thus, PSD and human exportin-t are more closely related to each other than either one is to Los1p. All three proteins have a conserved Ran-

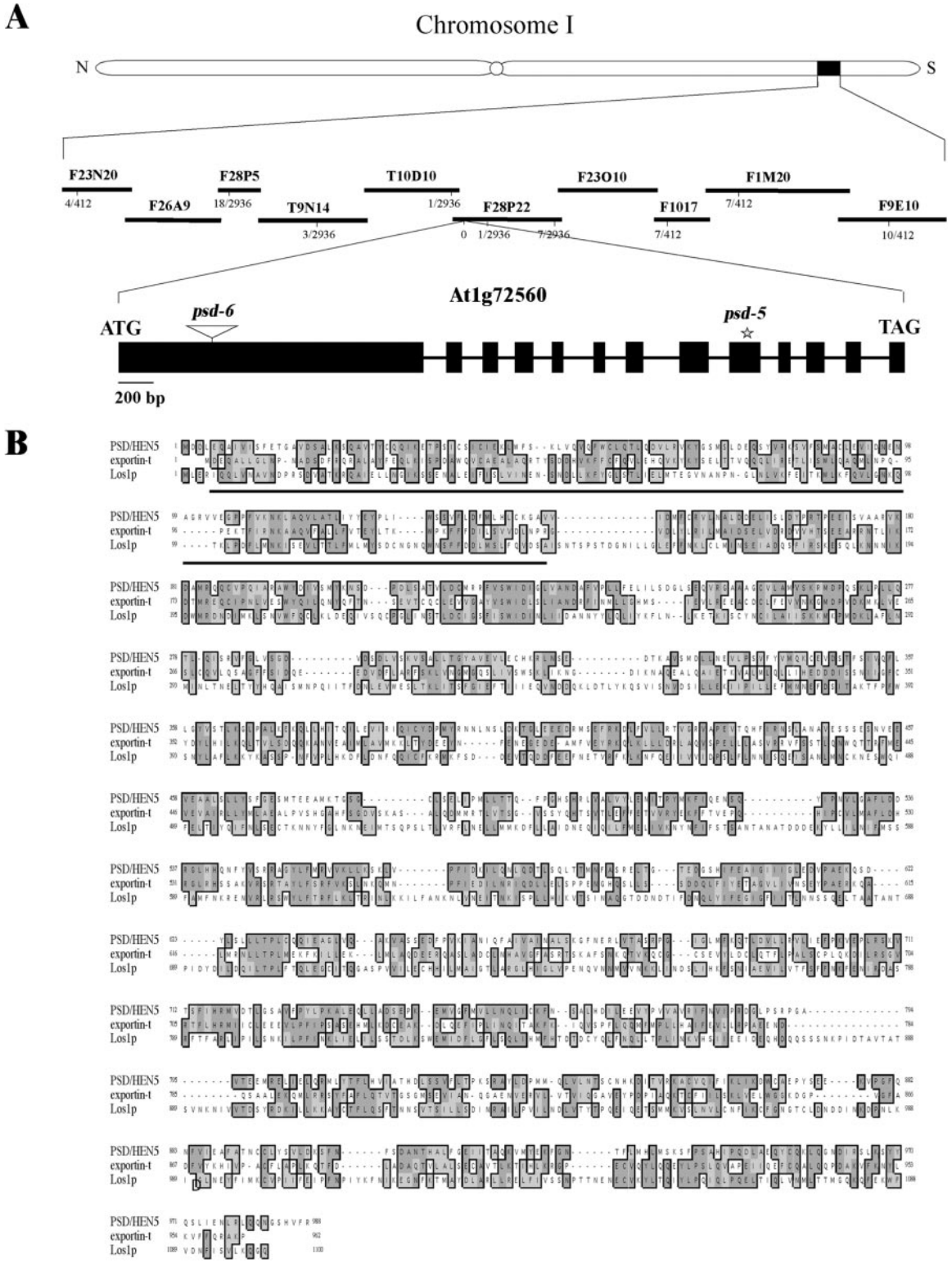

Figure 3. The *PSD* gene and protein. A, Positional cloning of *PSD*. The black lines represent BACs with the BAC names indicated above. The recombination frequencies at the markers (vertical lines) are shown below the BACs as number recombination/number chromosome. The *PSD* genomic structure is shown with rectangles representing exons and lines representing introns. The *psd-5* single nucleotide deletion is marked as a star in exon 9 and the *psd-6* T-DNA insertion mutation is represented as an inverted triangle in exon 1. B, A clustalW alignment of PSD protein with exportin-t (human, *Homo sapiens*) and Los1p (*Saccharomyces cerevisiae*). The amino acids showing identity and ones showing similarity are outlined, and highlighted in dark and light gray, respectively. The lines below the alignment denote the Ran-binding domain.

binding domain, a signature of the importin-β protein family, at the N terminus of the proteins (Fig. 3B). No other proteins with comparable similarity with exportin-t and Los1p exist in the Arabidopsis genome. Therefore, PSD is most likely a unique ortholog of exportin-t in Arabidopsis and possibly acts in the nucleocytoplasmic transport of tRNA in a Ran-dependent manner.

Expression of A, B, and C genes in *hua1-1 hua2-1 psd-5*

We examined the expression of a class A gene *APETALA1* (*AP1*), the two class B genes *APETALA3* (*AP3*) and *PISTILLATA* (*PI*), and the class C gene *AG* in *hua1-1 hua2-1* and *hua1-1 hua2-1 psd-5* flowers to begin to understand the molecular basis of the homeotic transformation in *hua1-1 hua2-1 psd-5*. Consistent with the observed stamen-to-petal transformation in the third whorl and carpel-to-sepal transformation in the fourth whorl of *hua1-1 hua2-1 psd-5* flowers, *AP1* RNA was present in the inner two whorls (Fig. 4, A and B). Despite the fact that *hua1-1 hua2-1 psd-5* flowers showed loss-of-C function phenotypes, *AG* RNA was readily detected in the inner two whorls (Fig. 4, C and D). We did not detect any difference in the temporal or spatial patterns of *AG* expression between *hua1-1 hua2-1* and *hua1-1 hua2-1 psd-5* (Fig. 4, C and D, and data not shown). The class B gene *PI* also showed similar expression patterns in the two genotypes (data not shown). Interestingly, although *AP3* RNA was found exclusively in whorls 2 and 3 in *hua1-1 hua2-1* flowers (Fig. 4E), *AP3* RNA was detected in some cells on the adaxial side of the ovary in *hua1-1 hua2-1 psd-5* flowers (Fig. 4F). This suggests a factor that acts to restrict the expression of *AP3* from ovary cells in the fourth whorl is affected by mutations in PSD, a putative exportin-t.

PSD Is Required for Multiple Processes in Flower Development

We introduced mutations in the class A, B, or C genes into the *hua1-1 hua2-1 psd-5* background to further determine whether PSD, as a putative exportin-t, specifically affects the class C pathway in flower development. Although the phenotypes of *hua1-1 hua2-1 psd-5 ap2-2*, *hua1-1 hua2-1 psd-5 pi-3*, or *hua1-1 hua2-1 psd-5 ag-1* flowers indicate that primarily C function is affected in *hua1-1 hua2-1 psd-5* flowers, the *hua1-1 hua2-1 psd-5 ap1-1* combination revealed that *psd-5* also affects an earlier step in floral patterning. The finding that *psd-5* results in multiple developmental defects in the flower is consistent with the molecular role of PSD as a putative exportin-t.

hua1-1 hua2-1 psd-5 ap2-2

hua1-1 hua2-1 ap2-2 flowers resemble *ap2-2* flowers in the outer three whorls and *hua1-1 hua2-1* flowers in the fourth whorl (Chen and Meyerowitz, 1999; Fig. 2N). The *hua1-1 hua2-1 psd-5 ap2-2* quadruple mutant differed from *hua1-1 hua2-1 ap2-2* in that it had flowers with leaf-like organs in the outer three whorls and sepaloid carpels in the fourth whorl (Fig. 2O). This phenotype resembles that of *ag-1 ap2-2* (Bowman et al., 1991) and is consistent with the assumption that *hua1-1 hua2-1 psd-5* plants are compromised in class C function in the flower.

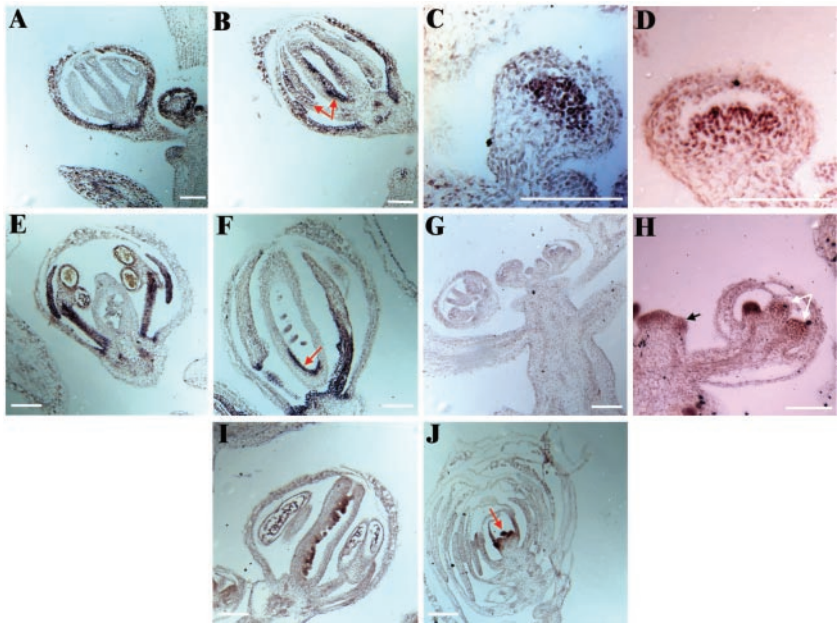

Figure 4. *AP1*, *AG*, *AP3*, and *PSD* RNA accumulation as determined by in situ hybridization. The brown/purple color represents positive hybridization signals. A, A stage 12 *hua1-1 hua2-1* flower without *AP1* expression in the inner two whorls. B, A *hua1-1 hua2-1 psd-5* flower with ectopic *AP1* expression in the inner two whorls (arrows). C, A stage 5–6 *hua1-1 hua2-1* flower showing *AG* RNA in the center. D, A stage 6 *hua1-1 hua2-1 psd-5* flower showing *AG* RNA in the center. E, A stage 12 *hua1-1 hua2-1* flower with *AP3* expression in the second and third whorls. F, A stage 12 *hua1-1 hua2-1 psd-5* flower showing ectopic expression of *AP3* on the adaxial side of the ovary (arrow). G, A longitudinal section of an L*er* inflorescence hybridized to a *PSD* sense probe. H through J, Hybridization of L*er* (H and I) and *ag-1* (J) tissues to a *PSD* antisense probe. *PSD* expression can be detected in young stamens and carpels (white arrows) in a stage 10 flower and in young floral meristems (black arrow; H), in the ovules of a stage 12 flower (I) and in the central young floral organs and the meristem (arrow) in the *ag-1* flower (J). Size bar = 50 μm.

hua1-1 hua2-1 psd-5 pi-3

pi-3 is a week allele with sepals in the outer two whorls and carpels in the inner two whorls (Bowman et al., 1991). *hua1-1 hua2-1* enhances the *pi-3* phenotype such that the third whorl organs in *hua1-1 hua2-1 pi-3* show reduced carpel character and develop into sepals, carpelloid sepals, and/or filaments (Chen and Meyerowitz, 1999; Fig. 2P). The third whorl phenotype of *hua1-1 hua2-1 pi-3* was further enhanced by *psd-5*, such that only sepals were present in the third whorl of *hua1-1 hua2-1 psd-5 pi-3* flowers (Fig. 2Q). The lack of carpel characteristics in the third whorl of *hua1-1 hua2-1 psd-5 pi-3* flowers is consistent with the assumption that class C activity is greatly reduced in *hua1-1 hua2-1 psd-5*.

hua1-1 hua2-1 psd-5 ag-1

hua1-1 hua2-1 ag-1 flowers resemble those of *ag-1* (Chen and Meyerowitz, 1999; Fig. 2L). *hua1-1 hua2-1 psd-5 ag-1* quadruple mutants were indistinguishable from *hua1-1 hua2-1 ag-1* triple mutants in terms of the homeotic transformation defects in the third whorl or the floral determinacy defects in the fourth whorl (Fig. 2M), indicating that *ag-1* is epistatic to *psd-5*.

hua1-1 hua2-1 psd-5 ap1-1

ap1-1 is a severe loss of function mutation in the class A gene *AP1* (Irish and Sussex, 1990; Bowman et al., 1993). In addition to its role in floral organ identity specification, *AP1* also specifies floral meristem identity (Mandel et al., 1992; Mandel and Yanofsky, 1995). *hua1-1 hua2-1 ap1-1* flowers resemble *ap1-1* flowers (Chen and Meyerowitz, 1999; Fig. 2R). We generated the *hua1-1 hua2-1 psd-5 ap1-1* quadruple mutant to determine whether the ectopic *AP1* expression in the third whorl of *hua1-1 hua2-1 psd-5* flowers was responsible for the stamen-to-petal transformation. The introduction of *ap1-1* into *hua1-1 hua2-1 hen4-1*, which has petals in the third whorl, rescued the third whorl defect of *hua1-1 hua2-1 hen4-1* such that stamens were found in the quadruple mutant (Cheng et al., 2003). However, *hua1-1 hua2-1 psd-5 ap1-1* plants showed a novel phenotype. The quadruple mutant "flowers" resembled shoots in that they contained sepal/leaf-like organs with a spiral phyllotaxy and a few carpelloid organs in the center (Fig. 2S). The lack of recognizable third whorl organs in the quadruple mutants prevented the assessment of the role of *AP1* in the stamen-to-petal transformation in the third whorl of *hua1-1 hua2-1 psd-5* flowers. However, the novel phenotype suggests that *psd-5* not only affects C function in flower development, but also affects an earlier activity, which specifies the identity of the floral meristem or to allow its proper development. This is consistent with the observation that *psd-5* also enhanced the floral meristem defects of *lfy* mutants (see below).

PSD Is Required for the Specification or Proper Development of the Floral Meristem

psd mutants had slightly more cauline leaves than wild type (data not shown), a phenotype that suggests delayed transition of the SAM from generating shoots to making flowers. To elucidate the possible requirement for *PSD* in the process of shoot-to-flower transition, we generated *psd-5 lfy-5* and *psd-5 lfy-6* double mutants. *LEAFY* (*LFY*) confers floral meristem identity and transcriptionally activates various floral homeotic genes (Weigel et al., 1992; Mandel and Yanofsky, 1995; Weigel and Nilsson, 1995; Busch et al., 1999; Wagner et al., 1999; Lamb et al., 2002). *lfy-6*, a strong *lfy* allele, produces flowers subtended by bracts and early flowers with leaf-like organs arranged in a spiral instead of a whorled pattern, suggesting loss of floral identity and gain of inflorescence shoot characteristics (Weigel et al., 1992). Most of the floral organs in later flowers are sepaloid or carpelloid organs (Weigel et al., 1992; Fig. 5D). In contrast to *lfy-6*, the weak *lfy-5* allele has flowers with more normal floral organs (Weigel et al., 1992; Fig. 5A) and is fertile. Nevertheless, *lfy-5* also displays defects in shoot-to-flower transition (Weigel et al., 1992). *psd-5* enhanced the phenotypes of *lfy-5* and *lfy-6* in terms of production of flowers from the SAM. *psd-5 lfy-6* plants were similar to *psd-5* until the stage of flower generation. After a few cauline leaves emerged, the primary inflorescence developed a number of lateral outgrowths with unknown identities (data not shown) and then terminated in a carpel-like structure with stigmatic tissue (Fig. 5E) or in filaments (Fig. 5F). The lateral outgrowths never developed further to flowers or any structures other than filaments (Fig. 5, E and F). Like in *psd-5 lfy-6*, the primary inflorescence in *psd-5 lfy-5* plants also produced lateral outgrowths that lacked apparent differentiation (Fig. 5, B and C). The synergistic interaction of *psd-5* and *lfy* and the absence of most floral organs in *hua1-1 hua2-1 psd-5 ap1-1* plants (Fig. 2S) indicate a requirement for *PSD* in floral meristem identity specification or in the subsequent development of the floral meristem after its identity has been correctly specified.

PSD Is Required for _AG_ Expression

To determine the molecular basis of the floral phenotypes of *hua1-1 hua2-1 psd-5* plants, we examined the expression of *AG* at the RNA and protein levels. *HUA1* and *HUA2* are required for the proper processing of *AG* pre-mRNA (Cheng et al., 2003). Aberrant *AG* RNAs with part of the *AG* second intron were produced in *hua1-1 hua2-1* flowers (Cheng et al., 2003; Fig. 6A). The levels of *AG* mRNA and aberrant *AG* RNA were reduced approximately 25% in *hua1-1 hua2-1 psd-5* as compared with *hua1-1 hua2-1* (Fig. 6A). Similarly, *AG* mRNA accumulation was reduced by approximately 22% in *psd-6* as compared with

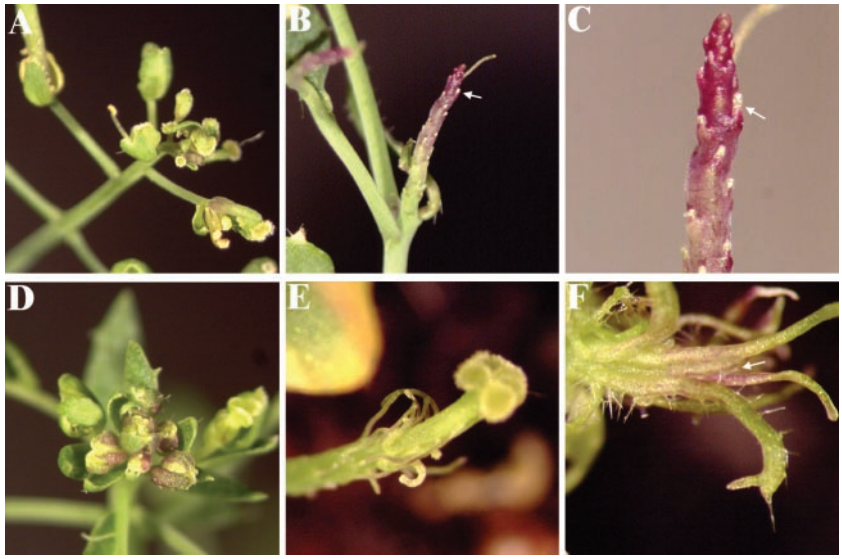

Figure 5. Interactions between *psd* and *lfy*. A, A *lfy-5* inflorescence with flowers. B, A *psd-5 lfy-5* primary inflorescence (arrow) without the formation of flowers. C, A magnification of the inflorescence stem in B. Outgrowths that appear undifferentiated (arrow) are found along the stem and the internodes are more compact than those in *lfy-5*. D, A *lfy-6* inflorescence with abnormal flowers lacking petals and stamens. E, A *psd-5 lfy-6* inflorescence, which produces filamentous organs at positions normally occupied by flowers and terminates in a structure with stigmatic tissues at the top. F, A *psd-5 lfy-6* inflorescence terminating in filamentous organs that sometimes have two-branched trichomes (arrow), suggesting that the organs have leaf character.

wild type (Col; Fig. 6A). Thus, we conclude that *PSD* is required for the accumulation of *AG* mRNA and likely acts independently of *HUA1* and *HUA2* because *psd-5* did not result in an increase in the level of aberrant *AG* RNAs. Considering that PSD is the ortholog of exportin-t, it is likely that the expression of a positive regulator of *AG* is reduced below a threshold level by *psd* mutations. Previous studies showed that 40% to 50% of wild-type *AG* mRNA levels could result in flowers with floral homeotic and determinacy defects similar to those in *hua1-1 hua2-1 psd* flowers (Mizukami and Ma, 1995; Cheng et al., 2003). Therefore, the reduced *AG* mRNA level in *hua1-1 hua2-1 psd-5* can be sufficient to result in its floral phenotypes.

We also examined AG protein accumulation in wild-type and various *psd* mutants. AG protein was readily detected in *psd-5*, *psd-6* (L*er*), and *psd-6* (Fig. 6B), although the levels of AG, relative to PEP carboxylase, may be slightly reduced in the *psd* single mutants as compared with the wild-type controls. This was largely consistent with the slight reduction of *AG* mRNA levels in *psd* single mutants. However, a dramatic difference in AG protein levels was detected between *hua1-1 hua2-1 psd-5* and *hua1-1 hua2-1*, although the difference at the *AG* mRNA level was not as great. This suggests that *PSD* may contribute to *AG* expression at the translational or posttranslational levels. Because *PSD* encodes a putative tRNA nuclear export receptor, it is likely that the low level of AG protein in *hua1-1 hua2-1 psd-5* results from defects in *AG* RNA translation. The fact that the effect of *psd* mutations on AG protein level is only obvious in the *hua1-1 hua2-1* background could be due to the reduced *AG* RNA level in *hua1-1 hua2-1*, which may cause *AG* RNA translation to be more sensitive to global perturbation in protein synthesis.

Expression of *PSD* in Plants

PSD was expressed in seedlings, leaves, stems, and inflorescences as determined by RNA filter hybridization (Fig. 7). Several forms of *PSD* RNA were detected. The major one corresponded in size to the full-length mRNA (approximately 3 kb) and constituted more than 75% of total *PSD* RNA. The molecular nature of the smaller RNA species, which were less abundant, was unclear. They were unlikely degraded *PSD* RNA from RNA isolation because the same RNA samples did not show degradation of *UBQ5* RNA. We also examined the accumulation of *PSD* RNA in different mutants (Fig. 7). Similar levels of *PSD* RNA in L*er* and *hua1-1 hua2-1* were found, suggesting that *PSD* is not regulated by *HUA1* or *HUA2. PSD* RNA abundance was increased in *ag-1* inflorescences (Fig. 7), which may simply be due to the presence of more young floral organs in *ag-1* flowers (see below). No *PSD* RNA species were detected in *psd-6* inflorescence (Fig. 7), suggesting that *psd-6* is a complete loss-of-function allele and indicating that all the RNA species detected in RNA filter hybridization correspond to *PSD* RNA. The fact that the *psd-6* plants are viable and fertile suggests that there must be other proteins with a similar molecular function. Despite being a potentially more severe allele than *psd-5*, *psd-6* results in less severe vegetative defects compared with *psd-5*. This is likely due to the presence of genetic modifiers in the two different ecotypes because *psd-6* (L*er*), which was derived from two backcrosses of *psd-6* to L*er*, appeared very similar to *psd-5* in terms of the vegetative phenotypes.

We examined *PSD* RNA expression patterns in flowers by in situ hybridization with a probe corresponding to the first exon of the *PSD* gene. *PSD* RNA was detected in all four types of young floral organs (Fig. 4, G–I and data not shown). Expression in stages

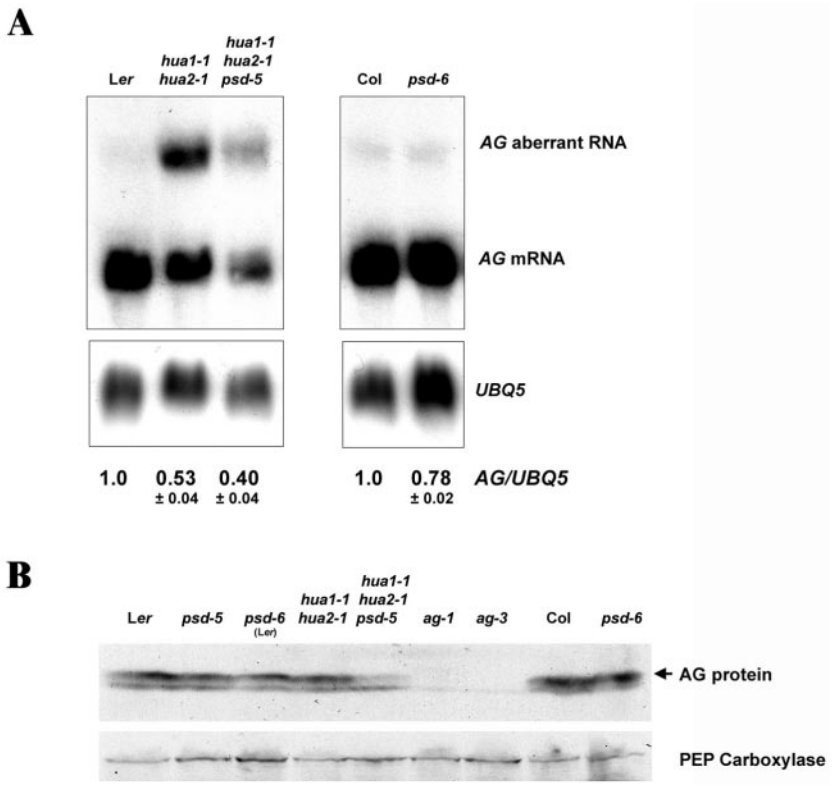

Figure 6. *AG* RNA and protein accumulation. A, *AG* RNA accumulation in various genetic backgrounds as determined by RNA filter hybridization (top panel). The same blot was hybridized with *UBQ5* for comparison (bottom panel). The numbers shown below indicate the relative abundance of *AG* mRNA among different genotypes. These numbers were derived from statistical analysis of three independent experiments. Note that although some hybridization signals may appear saturated in this picture, the signal intensity was in the linear range of phosphorimager quantitation. B, AG protein accumulation in different genotypes (arrow, top panel) as determined by western blotting. As a loading and blotting control, phospho*enol*pyruvate (PEP) carboxylase (Kandasamy et al., 2002) accumulation is shown in the bottom panel. The *psd-6* (L*er*) strain was obtained by two backcrosses of *psd-6* (Col) to L*er*.

one to two floral meristems (Fig. 4H) was also detected, consistent with the role of *PSD* in floral meristem identity. Expression of *PSD* RNA was also examined in *ag-1* flowers. High levels of *PSD* RNA were detected in young internal flowers and in the meristems in the center of *ag-1* flowers (Fig. 4J). The abundance of young floral organs expressing *PSD* in *ag-1* flowers may explain the increased *PSD* RNA abundance in *ag-1* flowers (Fig. 7).

DISCUSSION

PSD Is Required in the SAM and Floral Meristems

The *hua1-1 hua2-1 psd-5* flowers have petals in the third whorl and sepaloid carpels or an internal flower in the fourth whorl, phenotypes that resemble those of *ag* mutants. *psd-5* single mutants exhibit occasional sepal cells in the valves of the gynoecium. These phenotypes suggest that *PSD* is required for C function in the flower. Unlike *HUA1* and *HEN4*, which seem to be specific for the class C pathway in flower development, *PSD* is required more broadly in flower development. This is reflected by the fact that *AP3* is misexpressed in *hua1-1 hua2-1 psd-5* but not *hua1-1 hua2-1* flowers, and that *psd-5* enhances the floral meristem identity defects of *ap1-1* and *lfy* mutants. As a putative tRNA export receptor, it is unlikely that PSD acts directly to specify the identities of the floral meristem or floral organ primordia. Instead, it is more likely that PSD is required for the proper expression of genes in the regulatory networks that specify these identities. The delayed leaf appearance in *psd* mutants may reflect a requirement for *PSD* in cell division and/or differentiation in the SAM or in the lateral primordia originated from the SAM. The fact that *psd-5* enhances *lfy* and *ap1* in floral meristem identity defects suggests that *PSD* is required for lateral meristems to adopt their proper identities or to develop properly. In fact, almost all vegetative and floral defects of *psd* mutants point to a role for *PSD* in tissues undergoing cell division

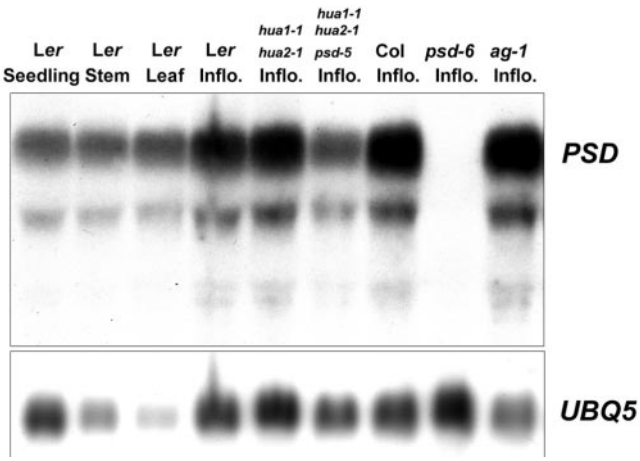

Figure 7. *PSD* RNA accumulation in total RNAs from different tissues and genotypes (top panel) as determined by RNA filter hybridization. The same blot was hybridized with a *UBQ5* probe for comparison (bottom panel). Inflo., Inflorescences.

and/or differentiation, such as the SAM, lateral meristems, or organ primordia. Consistent with this, in transgenic plants containing the *uidA* gene driven by the *PSD* promoter, β-glucuronidase (GUS) activity can be detected at high levels in regions undergoing fast cell division and/or differentiation, such as young leaf, growing leaf blades, young floral organs, and root tips (Supplemental Fig. 1 available at http://www.plantphysiol.org). In contrast, little GUS expression was detected in mature organs (Supplemental Fig. 1). In light of the fact that PSD is likely a tRNA export receptor, the *PSD* expression patterns and the *psd* mutant phenotypes may reflect more active tRNA export in meristems and young organs.

PSD Is Required for Proper Expression of Multiple Genes in Plant Development

The PSD protein is most probably the Arabidopsis ortholog of exportin-t and Los1p, nuclear receptors of tRNA export in humans and yeast, respectively. Hunter et al. (C. Hunter et al., 2003) showed that *PSD* rescued the *los1* mutant phenotype in yeast, suggesting that PSD can act in tRNA nuclear export. It is then reasonable to hypothesize that cytoplasmic tRNA abundance would decrease in *psd* mutants, leading to an overall reduced rate of translation and consequently lower level of protein accumulation. Such a potential molecular function of *PSD* is consistent with the fact that *PSD* is required in multiple processes in development. This model also predicts that expression of almost all proteins should be affected because the function of tRNA export is fundamental. However, although many developmental processes are affected in *psd* mutants, leaf formation and SAM organization in seedlings appear to be most sensitive to loss of *PSD* function. Floral organ identity defects are only found in the *hua1-1 hua2-1* background. We hypothesize that the apparent differential sensitivity of various developmental processes to loss of *PSD* activity may be due to the following reasons. First, *PSD* may not be required to the same extent for the expression of different proteins. Proteins required for SAM organization and leaf initiation may be affected more than other proteins by *psd* mutations. It was shown that the nuclear export of some tRNAs is not affected by *los1* mutations in yeast (Grosshans et al., 2000) and that all tRNA species may not be transported by human exportin-t (Bohnsack et al., 2002). Therefore, some proteins may be preferentially sensitive to defects in the nuclear export of a subset of tRNAs in *psd* mutants. This is consistent with our observation that AG abundance is more affected in *hua1-1 hua2-1 psd-5* than that of PEP carboxylase. Second, all proteins may be affected by *psd* mutations, but different developmental processes may require different threshold levels of their key regulator proteins such that some processes are more sensitive to reduction of protein abundance. Finally, the somewhat limited developmental defects of *psd* mutants may not reflect a differential effect of *psd* mutations on different cellular proteins, but rather a stronger requirement for tRNA export in actively growing tissues.

It is unknown what proteins are responsible for the various *psd* phenotypes, as a result of presumably globally reduced protein synthesis in *psd* mutants. The *psd* early seedling phenotypes are similar to that of *pinhead/zwille* mutants. *PINHEAD* (*PNH*)/*ZWILLE (ZLL)* is important for SAM formation and/or maintenance such that mutations in *PNH/ZLL* result in seedlings with terminal leaves (Moussian et al., 1998; Lynn et al., 1999), phenotypes also found in some *psd-5* plants. Therefore, decreased expression of *PNH/ZLL* in *psd* plants may cause the defects in seedling development. The translation of *AG* RNA is probably affected by *psd* mutations. This is supported by the observation that AG protein abundance is greatly reduced in *hua1-1 hua2-1 psd-5* compared with *hua1-1 hua2-1*, whereas the difference at the *AG* mRNA level is not so great. Expression of other gene(s) upstream of *AG* may also be directly facilitated by *PSD* because the *AG* mRNA level is reduced in *psd* single mutants compared with wild type. The reduced accumulation of *AG* RNA and protein is likely causing the homeotic phenotypes in *hua1-1 hua2-1 psd* flowers. *psd-5*, *hua1-1 psd-5*, and *hua2-1 psd-5* plants show reduced fertility. We presume that *psd-5* affects the expression of a gene or genes involved in fertility.

Redundant tRNA Export Pathway(s) in Arabidopsis

Because tRNA is an essential element required for translation, it would be expected that efficient tRNA export from the nucleus to the cytoplasm is essential for viability. However, Los1p, a tRNA exportin from yeast (Hellmuth et al., 1998; Sarkar and Hopper, 1998) is nonessential (Hurt et al., 1987), indicating that Los1p is dispensable for tRNA export in yeast and that there must be other tRNA export pathways. Several Los1p-independent pathways have been reported in yeast (Grosshans et al., 2000; Feng and Hopper, 2002), although none of the proteins found in these pathways seems to be a transport receptor, like Los1p, which is a member of the importin-β protein family (Görlich et al., 1997). The role of a mammalian importin-β protein, exportin-5, in tRNA export was recently reported (Bohnsack et al., 2002; Calado et al., 2002). Exportin-5, known previously to export double-stranded RNA-binding proteins (Brownawell and Macara, 2002), binds eukaryotic elongation factor 1A (eEF1A) via aminoacylated tRNAs and exports them out of the nucleus (Bohnsack et al., 2002; Calado et al., 2002). Here, we showed that plants are still viable even when *PSD* RNAs are completely depleted (i.e. in *psd-6*). This suggests that in Arabidopsis, as in yeast and mam-

mals, there may be redundant pathways for tRNA nuclear export. Arabidopsis has an exportin-5 homolog, namely HASTY, loss-of-function mutations in which cause defects in many different processes in plant development (Bollman et al., 2003). Although a role in nucleocytoplasmic transport has yet to be demonstrated, HASTY interacts with Ran in a yeast two-hybrid assay (Bollman et al., 2003), which is consistent with such a potential role. An alternative possibility is that passive diffusion of tRNAs through nuclear pores is sufficient for viability. Although not essential for viability, the defects of *psd* mutants indicate that *PSD* is necessary for multiple developmental processes in a multicellular organism.

MATERIALS AND METHODS

Plant Strains and Ethyl Methanesulfonate Mutagenesis

The strains used in this work are *hua1-1*, *hua2-1*, *hua1-1 hua2-1*, *hua1-1 hua2-1 ap1-1*, *hua1-1 hua2-1 ap2-2*, *hua1-1 hua2-1 pi-3*, *hua1-1 hua2-1 ag-1* (Chen and Meyerowitz, 1999), *lfy-5*, and *lfy-6* (Weigel et al., 1992) in the L*er* background. *psd-5*, in the L*er* background, and *psd-6*, in the Col background, were isolated in this study. *hua1-1* and *hua2-1* were introgressed into the Col background by crossing *hua1-1 hua2-1* to Col four times, resulting in *hua1-1 hua2-1* (Col). All plants were grown in Pro-mix BX (Premier, Quakertown, PA) under continuous light or long-day (16 h of light/8 h of dark) conditions at 23°C.

Ethyl methanesulfonate mutagenesis was performed as described previously (Chen et al., 2002). *DH677* is one of the M2 lines isolated, containing *psd-5*, *hua1-1*, and *hua2-1* mutations simultaneously. *psd-6* was identified by searching the Salk T-DNA insertion database and was obtained from the Arabidopsis Biological Resource Center. *psd-6* was backcrossed into the L*er* background twice before using in the analysis of AG protein accumulation.

RNA Filter and In Situ Hybridization

Total RNA was isolated with TRI-REAGENT solutions (Molecular Research Center, Cincinnatti). Approximately 50 μg of total RNA was loaded for each sample. RNA blotting and hybridization were carried out according to Li et al. (2001). Quantitation was performed with a Storm PhosphorImager (Molecular Dynamics, Sunnyvale, CA). The probe for detecting *AG* RNA was described previously as probe 1, which contains the *AG* full-length genomic region (Cheng et al., 2003). The *PSD* probe was amplified from the *PSD* cDNA with Exp1 (5′-atactaattcaaggcattgtttgacttgtatg-3′) and Exp2 (5′-ggttcgagtcggagaacatgattatg-3′).

In situ hybridization was carried out as described (Li et al., 2001). *AG*, *AP1*, *PI*, and *AP3* probes were as described (Chen et al., 2002). The plasmids making *PSD* probes were generated by amplifying a 1-kb *PSD* cDNA with HEN5p5 (5′-gcgcggagctcatggatgaccttgaacaggcaatagta-3′) and HEN5p18 (gcgcggagctcttcgttcagcaaatccatggaga-3′), and cloning them into pCR2.1-TOPO (Invitrogen, Carlsbad, CA) in two orientations. The resulting pCR2.1-TOPO-HEN5AS and pCR2.1-TOPO-HEN5S plasmids were in vitro transcribed to generate the antisense and sense probes.

SEM

Tissue fixation, critical point drying, and image acquisition for SEM were performed as described previously (Western et al., 2002).

Immunological Detection of Plant Proteins

Plant proteins were isolated and resolved in SDS-PAGE as described (Riechmann et al., 1999). Rabbit antisera that specifically recognize Arabidopsis AG protein were used (1:3,000) in the immunological detection of AG. Rabbit anti-PEP carboxylase (maize [*Zea mays*] leaf) polyclonal antibody (Rockland, Gilbertsville, PA) was used as a loading and electroblotting control. Blotting and detection were performed according to instructions from the enhanced chemiluminescence plus Western Blotting Detection System (Amersham Pharmacia Biotech, Piscataway, NJ).

Map-Based Cloning of *PSD*, Genomic Complementation, and cDNA Isolation

hua1-1 hua2-1 psd-5/+ plants were crossed with *hua1-1hua2-1* (Col), and the F_2 population segregating the *hua1-1 hua2-1 psd-5* floral phenotype was used as the mapping population, in which approximately 1,500 triple-mutant plants were identified. Genomic DNA was isolated as described (Edwards et al., 1991) from these F_2 mutant plants. SSLP markers were used to initially locate *PSD* to the bottom of chromosome I between markers nga280 and AthATPASE. SSLP and cleaved-amplified polymorphic sequence markers based on the Cereon L*er*/Col SNP database were used to further map *PSD* to a 27-kb region on the BAC of F28P22. Sequencing four candidate genes in this region revealed a single-nucleotide deletion mutation in At1g72560.

Approximately 7 kb of At1g72560 genomic region was amplified with HEN5p3 (5′-cggggtacctgatttgtagtctcatacgtgcgaatatacatt-3′) and HEN5p4 (5′-cggggtacccaattgtcaaaagaacaatctgtgtttgg-3′), and was cloned into the pPZP211 binary vector. The plasmid pPZP211-HEN5p3/4, or the control plasmid pPZP211-*35S-GFP*, was transformed into *psd-5 hua2-1* plants by the *Agrobacterium tumefaciens*-mediated infiltration method. The T_1 transgenic plants were selected on medium containing 50 μg mL^{-1} kanamycin.

Reverse transcription-PCR was performed on the total RNA isolated from L*er* inflorescence with HEN5p8 (5′-aaaactgcagctaatttgatctggatggtg-aaagcga-3′) and HEN5p11 (5′-aaaactgcagccatggatgaccttgaacaggcaatagtaatt-3′), which are located in the 5′- and 3′-untranslated regions, respectively. The amplified cDNA was cloned into pCR2.1-TOPO (Invitrogen) and sequenced. The sequence is in GenBank under the accession number AY288073.

PSD-GUS Expression Analysis

A 1.8-kb *PSD* genomic fragment upstream of ATG was amplified with HEN5p7 (5′-aaaactgcagtgatttgtagtctcatacgtgcgaatatacatt-3′) and HEN5p9 (5′-aaaactgcagtgtgttaacttaaccccactacaaaaaccc-3′), and was cloned into a pPZP211-GUS plant expression vector (Wang and X. Chen, unpublished data). The resulting pPZP211-*PSD-GUS* plasmid was transformed into L*er* plants. Transgenic plants were selected as described above. GUS staining was performed as described (Jefferson et al., 1987).

ACKNOWLEDGMENTS

We thank Yulan Cheng for the isolation of *psd-5* and for help with the initial mapping of *PSD*, Dr. Tamara western for introgressing *hua1-1 hua2-1* into Columbia, and Jiqun Zhao and Junhong Sun for assistance in the mapping and cloning of *PSD*. We also thank Drs. Nilgun Tumer, Randall Kerstetter, and Terri Kinzy for valuable suggestions on this work and Drs. Randall Kerstetter, Jun Liu, and Wonkeun Park for helpful comments on the manuscript. We acknowledge Cereon for the release of L*er*/Col SNP database and Salk Institute Genomic Analysis Laboratory (SIGnAL) and the Arabidopsis Biological Resource Center (ABRC) for the isolation and distribution of T-DNA insertion lines.

Received March 11, 2003; returned for revision April 24, 2003; accepted May 5, 2003.

LITERATURE CITED

Arts GJ, Fornerod M, Mattaj IW (1998) Identification of a nuclear export receptor for tRNA. Curr Biol **8:** 305–314

Bohnsack TM, Regener K, Schwappach B, Saffrich R, Paraskeva E, Hartmann E, Görlich D (2002) Exp5 exports eEF1A via tRNA from nuclei and synergizes with other transport pathways to confine translation to the cytoplasm. EMBO J **21:** 6205–6215

Bollman KM, Aukerman MJ, Park M-Y, Hunter C, Berardini TZ, Poethig RS (2003) HASTY, the *Arabidopsis* ortholog of exportin 5/MSN5, regulates phase change and morphogenesis. Development **130:** 1493–1504

Bowman JL, Alvarez J, Weigel D, Meyerowitz EM, Smyth DR (1993) Control of flower development in *Arabidopsis thaliana* by *APETALA1* and interacting genes. Development **119:** 721–743

Bowman JL, Smyth DR, Meyerowitz EM (1989) Genes directing flower development in *Arabidopsis*. Plant Cell **1:** 37–52

Bowman JL, Smyth DR, Meyerowitz EM (1991) Genetic interactions among floral homeotic genes of *Arabidopsis*. Development **112:** 1–20

Brownawell AM, Macara IG (2002) Exportin-5, a novel karyopherin, mediates nuclear export of double-stranded RNA binding proteins. J Cell Biol **156:** 53–64

Busch MA, Bomblies K, Weigel D (1999) Activation of a floral homeotic gene in *Arabidopsis*. Science **285:** 585–587

Calado A, Treichel N, Müller E, Otto A, Kutay U (2002) Exportin-5-mediated nuclear export of eukaryotic elongation factor 1A and tRNA. EMBO J **21:** 6216–6224

Chen X, Liu J, Cheng Y, Jia D (2002) *HEN1* functions pleiotropically in *Arabidopsis* development and acts in C function in the flower. Development **129:** 1085–1094

Chen X, Meyerowitz EM (1999) *HUA1* and *HUA2* are two members of the floral homeotic *AGAMOUS* pathway. Mol Cell **3:** 349–360

Cheng Y, Kato N, Wang W, Li J, Chen X (2003) Two RNA binding proteins, HEN4 and HUA1, act in the processing of *AGAMOUS* pre-mRNA in *Arabidopsis thaliana*. Dev Cell **4:** 53–66

Cullen BR (2000) Nuclear RNA export pathways. Mol Cell Biol **20:** 4181–4187

Edwards K, Johnstone C, Thompson C (1991) A simple and rapid method for the preparation of plant genomic DNA for PCR analysis. Nucleic Acids Res **19:** 1349

Feng W, Hopper AK (2002) A Los1p-independent pathway for nuclear export of intronless tRNAs in *Saccharomyces cerevisiae*. Proc Natl Acad Sci USA **99:** 5412–5417

Görlich D, Dabrowski M, Bischoff FR, Kutay U, Bork P, Hartmann E, Prehn S, Izaurralde E (1997) A novel class of RanGTP binding proteins. J Cell Biol **138:** 65–80

Görlich D, Kutay U (1999) Transport between the cell nucleus and the cytoplasm. Annu Rev Cell Dev Biol **15:** 607–660

Grosshans H, Hurt E, Simos G (2000) An aminoacylation-dependent nuclear tRNA export pathway in yeast. Genes Dev **14:** 830–840

Grosshans H, Simos G, Hurt E (2000) Transport of tRNA out of the nucleus-direct channeling to the ribosome. J Struct Biol **129:** 288–294

Hellmuth K, Lau DM, Bischoff FR, Kunzler M, Hurt E, Simos G (1998) Yeast Los1p has properties of an exportin-like nucleocytoplasmic transport factor for tRNA. Mol Cell Biol **18:** 6374–6386

Hunter C, Aukerman MJ, Sun H, Fokina M, Poethig RS (2003). *PAUSED* encodes the Arabidopsis exportin-7 orthologue. Plant Physiol **132:** 2135–2143

Hurt DJ, Wang SS, Li Y, Hopper AK (1987) Cloning and characterization of *LOS1*, a *Saccharomyces cerevisiae* gene that affects tRNA splicing. Mol Cell Biol **7:** 1208–1216

Irish VF, Sussex IM (1990) Function of the *apetala1* gene during *Arabidopsis* floral development. Plant Cell **2:** 741–753

Jefferson RA, Kavanagh TA, Bevan MW (1987) GUS fusions: β-glucuronidase as a sensitive and versatile gene fusion marker in higher plants. EMBO J **6:** 3901–3907

Kandasamy MK, Mckinney EC, Meagher RB (2002) Functional nonequivalency of actin isovariants in *Arabidopsis*. Mol Biol Cell **13:** 251–261

Kuersten S, Ohno M, Mattaj IW (2001) Nucleocytoplasmic transport: Ran, β and beyond. Trends Cell Biol **11:** 497–503

Kutay U, Lipowsky G, Izaurralde E, Bischoff FR, Schwarzmaier P, Hartmann E, Gorlich D (1998) Identification of a tRNA-specific nuclear export receptor. Mol Cell **1:** 359–369

Lamb RS, Hill TA, Tan QK, Irish VF (2002) Regulation of *APETALA3* floral homeotic gene expression by meristem identity genes. Development **129:** 2079–2086

Lenhard M, Bohnert A, Jürgens G, Laux T (2001) Termination of stem cell maintenance in *Arabidopsis* floral meristems by interactions between *WUSCHEL* and *AGAMOUS*. Cell **105:** 805–814

Li J, Jia D, Chen X (2001) *HUA1*, a regulator of stamen and carpel identities in *Arabidopsis*, codes for a nuclear RNA binding protein. Plant Cell **13:** 2269–2281

Lohmann JU, Hong RL, Hobe M, Busch MA, Parcy F, Simon R, Weigel D (2001) A molecular link between stem cell regulation and floral patterning in *Arabidopsis*. Cell **105:** 793–803

Lohmann JU, Weigel D (2002) Building beauty: the genetic control of floral patterning. Dev Cell **2:** 135–142

Lynn K, Fernandez A, Aida M, Sedbrook J, Tasaka M, Masson P, Barton MK (1999) The *PINHEAD/ZWILLE* gene acts pleiotropically in *Arabidopsis* development and has overlapping functions with the *ARGONAUTE1* gene. Development **126:** 469–481

Mandel MA, Gustafson-Brown C, Savidge B, Yanofsky MF (1992) Molecular characterization of the *Arabidopsis* floral homeotic gene *APETALA1*. Nature **360:** 273–277

Mandel MA, Yanofsky MF (1995) A gene triggering flower formation in *Arabidopsis*. Nature **377:** 522–524

Mizukami Y, Ma H (1995) Separation of *AG* function in floral meristem determinacy from that in reproductive organ identity by expressing antisense *AG* RNA. Plant Mol Biol **28:** 767–784

Moussian B, Schoof H, Haecker A, Jurgens G, Laux T (1998) Role of the *ZWILLE* gene in the regulation of central shoot meristem cell fate during *Arabidopsis* embryogenesis. EMBO J **17:** 1799–1809

Park W, Li J, Song R, Messing J, Chen X (2002) CARPEL FACTORY, a Dicer homolog, and HEN1, a novel protein, act in microRNA metabolism in *Arabidopsis thaliana*. Curr Biol **12:** 1484–1495

Riechmann JL, Ito T, Meyerowitz EM (1999) Non-AUG initiation of *AGAMOUS* mRNA translation in *Arabidopsis thaliana*. Mol Cell Biol **19:** 8505–8512

Sarkar S, Hopper AK (1998) tRNA nuclear export in *Saccharomyces cerevisiae*: in situ hybridization analysis. Mol Biol Cell **9:** 3041–3055

Telfer A, Bollman KM, Poethig RS (1997) Phase change and the regulation of trichome distribution in *Arabidopsis thaliana*. Development **124:** 645–654

Theissen G, Saedler H (2001) Floral quartets. Nature **409:** 469–471

Wagner D, Sablowski RW, Meyerowitz EM (1999) Transcriptional activation of *APETALA1* by *LEAFY*. Science **285:** 582–584

Weigel D, Alvarez J, Smyth DR, Yanofsky MF, Meyerowitz EM (1992) *LEAFY* controls floral meristem identity in *Arabidopsis*. Cell **69:** 843–859

Weigel D, Nilsson O (1995) A developmental switch sufficient for flower initiation in diverse plants. Nature **377:** 495–500

Western TL, Cheng Y, Liu J, Chen X (2002) HUA ENHANCER 2, a putative DExH-box RNA helicase, maintains homeotic B and C gene expression in *Arabidopsis*. Development **129:** 1569–1581